

Neuroprotective effects of autophagy inhibition on hippocampal glutamate receptor subunits after hypoxia-ischemia-induced brain damage in newborn rats

Li-xiao Xu^{1, #}, Xiao-juan Tang^{2, #}, Yuan-yuan Yang², Mei Li¹, Mei-fang Jin¹, Po Miao², Xin Ding², Ying Wang², Yan-hong Li², Bin Sun^{2, *}, Xing Feng^{2, *}

1 Institute of Pediatric Research, Affiliated Children's Hospital of Soochow University, Suzhou, Jiangsu Province, China

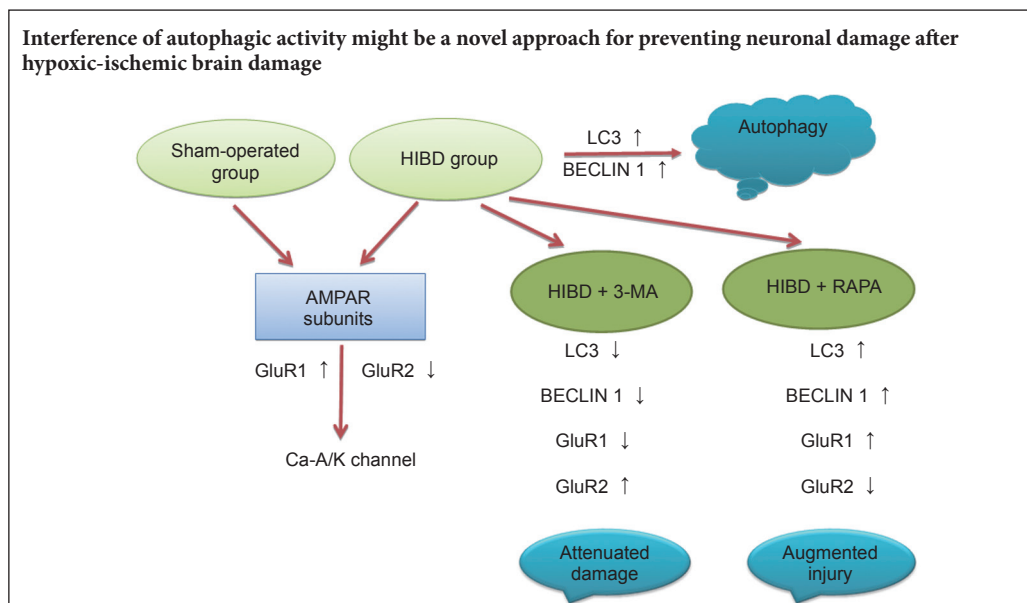
2 Department of Neonatology, Affiliated Children's Hospital of Soochow University, Suzhou, Jiangsu Province, China

How to cite this article: Xu LX, Tang XJ, Yang YY, Li M, Jin MF, Miao P, Ding X, Wang Y, Li YH, Sun B, Feng X (2017) Neuroprotective effects of autophagy inhibition on hippocampal glutamate receptor subunits after hypoxia-ischemia-induced brain damage in newborn rats. *Neural Regen Res* 12(3):417-424.

Open access statement: This is an open access article distributed under the terms of the Creative Commons Attribution-NonCommercial-ShareAlike 3.0 License, which allows others to remix, tweak, and build upon the work non-commercially, as long as the author is credited and the new creations are licensed under the identical terms.

Funding: This work was supported by the National Natural Science Foundation of China, No. 81471488, 81271378, 81502157, and 81501291; the Key Medical Subjects of Jiangsu Province of China, No. XK201120; the Jiangsu Province Key Research and Development of Special Funds in China, No. BE2015644; the Science and Technology Project of Suzhou City of China, No. SYSD2013105, SYS201446, SYS201441; the Public Health Technology Project of Suzhou City of China, No. SS201536; the Department of Pediatrics Clinical Center of Suzhou City of China, No. Szzx201504.

Graphical Abstract



*Correspondence to:

Bin Sun, Ph.D. or Xing Feng, Ph.D., sunyu0628@126.com or xing_feng66@suda.edu.cn.

#These authors contributed equally to this study.

orcid:

0000-0002-9756-9468 (Bin Sun)

doi: 10.4103/1673-5374.202945

Accepted: 2017-02-08

Abstract

Autophagy has been suggested to participate in the pathology of hypoxic-ischemic brain damage (HIBD). However, its regulatory role in HIBD remains unclear and was thus examined here using a rat model. To induce HIBD, the left common carotid artery was ligated in neonatal rats, and the rats were subjected to hypoxia for 2 hours. Some of these rats were intraperitoneally pretreated with the autophagy inhibitor 3-methyladenine (10 mM in 10 μ L) or the autophagy stimulator rapamycin (1 g/kg) 1 hour before artery ligation. Our findings demonstrated that hypoxia-ischemia-induced hippocampal injury in neonatal rats was accompanied by increased expression levels of the autophagy-related proteins light chain 3 and Beclin-1 as well as of the AMPA receptor subunit GluR1, but by reduced expression of GluR2. Pretreatment with the autophagy inhibitor 3-methyladenine blocked hypoxia-ischemia-induced hippocampal injury, whereas pretreatment with the autophagy stimulator rapamycin significantly augmented hippocampal injury. Additionally, 3-methyladenine pretreatment blocked the hypoxia-ischemia-induced upregulation of GluR1 and downregulation of GluR2 in the hippocampus. By contrast, rapamycin further elevated hippocampal GluR1 levels and exacerbated decreased GluR2 expression levels in neonates with HIBD. Our results indicate that autophagy inhibition favors the prevention of HIBD in neonatal rats, at least in part, through normalizing GluR1 and GluR2 expression.

Key Words: nerve regeneration; hypoxic-ischemic brain damage; hypoxia; ischemia; α -amino-3-hydroxy-5-methyl-4-isoxazolepropionic acid-type glutamate receptor subunit; GluR; hippocampus; rapamycin; 3-methyladenine; neural regeneration

Introduction

Neonatal hypoxic-ischemic encephalopathy is the leading cause of infant mortality and morbidity, affecting 1–2% of live full-term births (Perlman and Shah, 2011; Patel et al., 2014). Hypoxic-ischemic encephalopathy is a brain injury characterized by global hypoxia-ischemia as a result of inadequate oxygen and blood supply (Shankaran, 2012; Guo et al., 2016; Yao et al., 2016). Despite the development of emerging strategies for preventing hypoxic-ischemic brain damage (HIBD), undesirable adverse effects may occur following the application of required interventions, and alternative approaches with improved therapeutic effects are needed (Dixon et al., 2015; Zalewska et al., 2015).

A variety of factors and mechanisms have been implicated in the pathophysiology of HIBD, including vasculature changes, reduced oxygen and adenosine triphosphate supply, overload of Ca^{2+} influx, increased oxidative stress, mitochondrial dysfunction, chronic inflammation, and defective synaptogenesis and neurogenesis (Dixon et al., 2015). Autophagy is a highly conserved cellular degradative pathway by which intracellular molecules, proteins, and damaged organelles are delivered into lysosomes and degraded for recycling (Klionsky et al., 2016). A recent report has shown enhanced autophagic activity in the lentiform nucleus of human newborns who died of hypoxic-ischemic encephalopathy (Xie et al., 2016). In addition, the selective deletion of a key autophagy-related gene, *Atg7*, prevented HIBD-induced neuronal death in a mouse model (Xie et al., 2016). These data highlight the functional role of autophagy in mediating brain damage after hypoxic-ischemic injury. Nevertheless, the mechanisms underlying this role remain unclear.

Increased Ca^{2+} influx through α -amino-3-hydroxy-5-methyl-4-isoxazolepropionic acid-type (AMPA-type) glutamate receptor (AMPA) channels, especially Ca^{2+} -permeable AMPAR channels, also contributes to neuronal death in hypoxic-ischemic encephalopathy (Tang and Xing, 2013). Ca^{2+} -permeable AMPARs are composed of four subunits, GluR1, GluR2, GluR3, and GluR4, that form a tetraheteromeric structure (Liu and Savtchouk, 2012). In the hippocampus, a majority of neurons contain a heteromeric complex that consists of GluR1/GluR2 or GluR2/GluR3 (Shi et al., 2001). The accumulation of GluR1 and GluR2 subunits in synapses is required for mediating synaptic plasticity (Shi et al., 2001; Gainey et al., 2009). AMPARs have been found in autophagosomes in hippocampal neurons *in vitro* and *in vivo* (Matsuda et al., 2008). In addition, autophagy has been found to be responsible for the degradation of the GluR1 subunit in hippocampal neurons (Shehata et al., 2012).

Based on the aforementioned evidence, we speculated that AMPARs may participate in the pathogenesis of HIBD. Hence, we investigated here for the first time the effects of autophagy in mediating the expression of AMPARs (GluR1 and GluR2) in a rat model of HIBD. Based on the aforementioned evidence, we further investigated the contribution of AMPARs to the pathogenesis of HIBD.

Materials and Methods

Animals

Seven-day-old male and female Sprague-Dawley rats, weighing 11–14 g, were provided by Shanghai SLAC Laboratory Animal Co., Ltd., China (License No. SCXK [Hu] 2012-0002). These neonatal animals were breast-fed and housed at $25 \pm 2^\circ\text{C}$ with a 12-hour light/dark lighting cycle. The protocols, which included all surgical procedures and animal use, were approved by the Animal Care and Use Committee of Soochow University, and conformed to the Guide for the Care and Use of Laboratory Animals by the National Institutes of Health. Rats were randomly divided into the following four groups having 42 rats in each group: sham-operated, HIBD only, HIBD + 3-methyladenine (3-MA), and HIBD + rapamycin.

Establishing an animal model of HIBD in newborn rats

An animal model of HIBD was established in neonatal rats as previously described (Vannucci and Vannucci, 1997) with minor modifications. Briefly, rats were anesthetized using diethyl ether inhalation and placed in the supine position. A 1-cm midline incision of the neck was made to expose the left common carotid artery, which was permanently ligated using 7-0 suture. The incision was closed, and rats were placed in an incubator at 37°C for 2 hours. The rats were transferred to a normobaric hypoxia cabin (37°C , 8% O_2 , 92% N_2 , gas flow rate of 1.5 L/min; Shanghai Institute for Pediatric Research, China) for 2 hours to induce hypoxia. The time at the end of hypoxia induction was considered 0 hours. The neonates were returned to their home cages. In the sham-operated group, the left common carotid artery was exposed but not ligated. After the operation, the incision was sutured, and the sham-operated rats were kept in an incubator at 37°C without induction of hypoxia.

Drug administration

In the HIBD + 3-MA and HIBD + rapamycin groups, rats were intraperitoneally injected with 10 μL of 3-MA (10 mM; Sigma-Aldrich, St. Louis, MO, USA; an autophagy inhibitor) or 1 g/kg of rapamycin (5 mg/mL; Sigma-Aldrich; an autophagy stimulator), respectively. One hour after drug administration, the operation was conducted in these rats to induce HIBD. In both the sham-operated and HIBD only groups, rats were intraperitoneally injected with 10 μL of sterilized phosphate-buffered solution (PBS) 1 hour prior to surgery.

Brain swelling detected by brain wet weight

Rats were randomly selected from the sham-operated group and each of the three HIBD groups ($n = 6$ for each group). Twenty-four hours after the establishment of HIBD, rats were sacrificed and the left hemisphere of the brain was weighed.

Specimen collection

At 0, 1, 3, 6, 12, 24, or 48 hours after the operation, three rats from each group were decapitated. The brains were removed and fixed in 4% paraformaldehyde for histological examination. At 0, 1, 24, and 48 hours after the operation, six rats from each group were decapitated, and hippocampal tissues were collected and stored at -80°C until use.

Hematoxylin-eosin staining

Paraformaldehyde-fixed brain samples were incubated in 30% sucrose solution for 72 hours. After being embedded in paraffin, the samples were sectioned, deparaffinized in xylene, and rehydrated in a graded series of ethanol (100%, 95%, 85%, and 75%). The sections were stained with hematoxylin and eosin for histological examination. Five fields were randomly selected from each sample for analysis, and images were captured using a light microscope (OLYMPUS IX71; Olympus Corporation, Tokyo, Japan) at a magnification of $\times 400$.

Nissl staining

Brain sections (5 μm thick) were incubated with Nissl staining solution for 10 minutes at room temperature. Samples were then dehydrated through a graded series of ethanol (75%, 95%, and 100%), cleared in xylene, and mounted with neutral balsam. For each sample, three fields in the hippocampal region were randomly captured with a light microscope at a magnification of $\times 400$. The number of Nissl-positive hippocampal neurons in an area 1 mm \times 1 mm square was counted. The average number of hippocampal neurons was calculated from 18 randomly selected regions for each group.

Reverse transcription quantitative polymerase chain reaction (RT-qPCR)

Total RNA was extracted from hippocampal tissues using Trizol reagent (Invitrogen, Carlsbad, CA, USA) according to the manufacturer's instructions. Total RNA (2 μg) was reverse transcribed into cDNA. The PCR primers were synthesized by Sangon Biotech, Shanghai, China. Primer sequences used for PCR were as follows: light chain 3 (LC3), forward, 5'-ATC AAC ATT CTG ACG GAG CG-3'; reverse, 5'-TGC TTG GCA TCA AAC ACG-3'; bedin1, forward, 5'-TTC AAG ATC CTG GAC CGA GTG AC-3'; reverse, 5'-AGA CAC CAT CCT GGC GAG TTT C-3'; glur1, forward, 5'-CTC AAG CGT CCA GAA TAG G-3'; reverse, 5'-CAA GTC GGT AGG AGT AGC C-3'; glur2, forward, 5'-TGT GTT TGT GAG GAC TAC CGC A-3'; reverse, 5'-GGA TTC TTT GCC ACC TTC ATT C-3'; β -actin, forward, 5'-CCC ATC TAT GAG GGT TAC GC-3'; reverse, 5'-TTT AAT GTC ACG CAC GAT TTC-3'. The PCR reaction system included 2 μL of template cDNA, 1 μL of forward primer, 1 μL of reverse primer, 10 μL of 2 \times SYBR Green PCR Master Mix, and 6 μL of deionized water for a final volume of 20 μL . The reaction was conducted using a quantitative real-time PCR instrument with fluores-

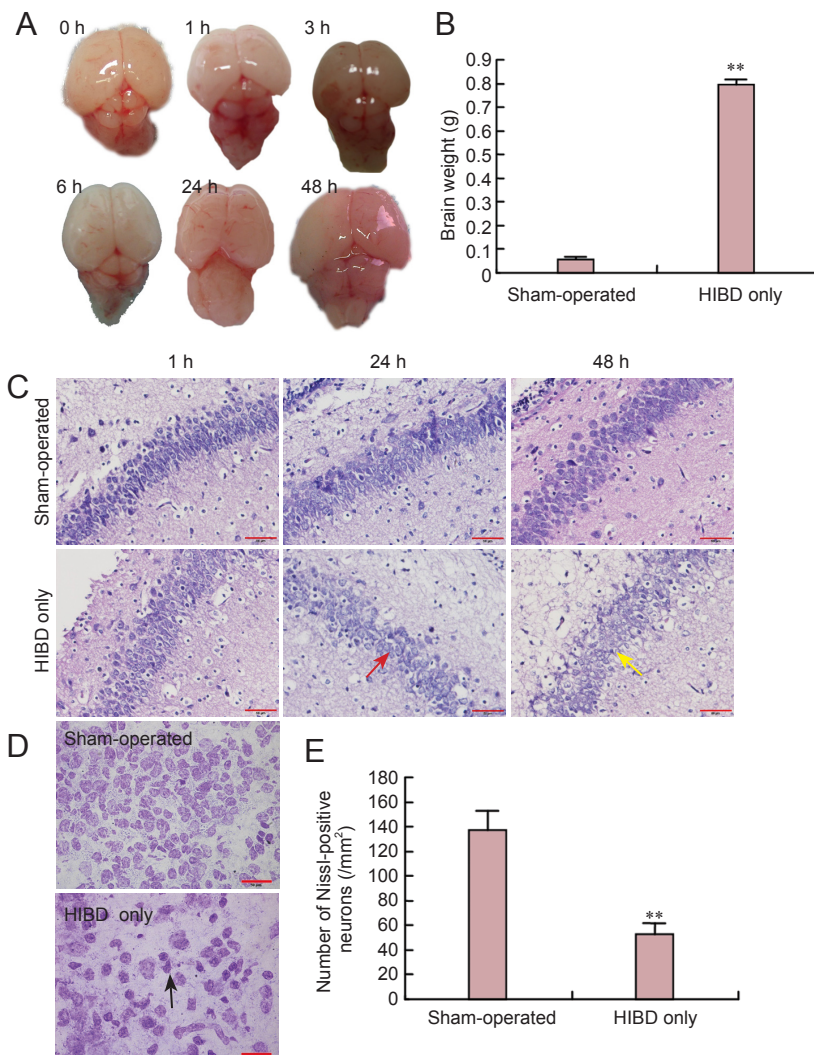


Figure 1 Pathological changes induced by hypoxia-ischemia in hippocampi of newborn rats.

(A) Gross and histological examinations of the brain following HIBD. The brains were removed and gross morphology examined at the indicated times after HIBD. (B) Brain wet weight was determined 24 h after establishing a rat model of HIBD ($n = 6$ for each group). (C) Brain sections were stained with hematoxylin-eosin (magnification, $\times 400$). In the sham-operated group, hippocampal neurons are conical or round, dense, and regular; the nucleus is centered and fully transparent. Only a small amount of neuronal degeneration or apoptosis is visible. In the HIBD group, hippocampal neurons display incomplete structure, disordered arrangement, fuzzy outlines, and unclear boundaries. Cell swelling, rupture and loss are observed. Neurons are loosely distributed, with increased cell spacing. Cell edema gradually increases with time. Red arrow indicates that hippocampal neurons have incomplete cell structure, disorderly arrangement, and blurred cell boundaries. Yellow arrow indicates that hippocampal neurons are swollen, broken, distributed loosely, and have increased cell spacing. (D) Nissl staining in the hippocampus 48 h after HIBD ($\times 400$) shows hippocampal structural damage, neuronal loss, nuclear fragmentation, and Nissl body damage. Arrow indicates positive Nissl staining. Scale bars in C and D: 50 μm . (E) The number of Nissl-positive hippocampal neurons in a region 1 mm \times 1 mm was counted 48 h after HIBD. Data are expressed as the mean \pm SD and were analyzed by one-way analysis of variance followed by the least significant difference test. ** $P < 0.01$, vs. sham-operated group. h: Hour(s). HIBD: hypoxic-ischemic brain damage.

cence detection (Roche LightCycler 480, Basel, Switzerland) under the following conditions: pre-denaturation at 95°C for 10 minutes, denaturation at 95°C for 15 seconds, annealing at 60°C for 15 seconds, and extension at 72°C for 30 seconds for a total of 50 cycles. The relative expression of mRNA was calculated using the $2^{-\Delta\Delta CT}$ method, with β -actin as an internal control (Livak and Schmittgen, 2001).

Immunohistochemistry

Paraffin-embedded tissue sections were boiled in citrate buffer (pH 6.0) for antigen retrieval. After being rinsed in PBS, the samples were incubated in 3% hydrogen peroxide at 37°C for 30 minutes, and blocked in goat serum followed by primary antibody incubation at 4°C overnight. The following primary antibodies were used: rabbit polyclonal anti-LC3 (1:200; Cell Signaling Technology, Beverly, MA, USA), rabbit Beclin 1 (1:150; Cell Signaling Technology), rabbit polyclonal anti-GluR1 (1:150; Sigma-Aldrich), and rabbit polyclonal anti-GluR2 (1:250; Sigma-Aldrich). After being incubated at 4°C overnight, the sections were rinsed with PBS and probed with a biotinylated secondary anti-rabbit antibody (ZSJQ-Bio, Beijing, China) for 1 hour at room temperature, followed by treatment with streptavidin conjugated to horseradish peroxidase. The samples were visualized with 3,3'-diaminobenzidine tetrahydrochloride. Nuclei were counterstained with hematoxylin. After mounting with neutral balsam, the samples were examined under a standard DP71 light microscope (Olympus, Monolith, Japan). Five fields were randomly selected from each section, and micrographs were captured at a magnification of $\times 200$.

Western blot assay

The hippocampal tissues were lysed in lysis buffer (Beyotime Institute of Biotechnology, Haimen, China). After centrifugation at $13,800 \times g$ for 5 minutes at 4°C, the supernatant was collected. Protein samples were separated by 8% or 10% sodium dodecyl sulfate-polyacrylamide gel electrophoresis. After being transferred onto a polyvinylidene fluoride membrane (0.45 μ m; Millipore, Billerica, MA, USA), the samples were blocked with 5% non-fat dry milk for 1 hour at room temperature and then incubated at 4°C overnight with the following primary antibodies: rabbit anti-GluR1 (1:2,000; Cell Signaling Technology), rabbit anti-GluR2 (1:500; Cell Signaling Technology), and mouse anti- β -actin (1:3,000; Santa Cruz Biotechnology, Santa Cruz, CA, USA). After being rinsed with Tris-buffered saline plus Tween 20 (0.1% Tween 20) three times, the membrane was incubated with secondary antibody against rabbit or mouse IgG conjugated to horseradish peroxidase (1:4,000; Cell Signaling Technology) for 1 hour at room temperature, and treated with enhanced chemiluminescence reagent (Beyotime Institute of Biotechnology). Blots were imaged using X-ray film (Eastman Kodak Co., USA), and images were captured using a scanner (Canon, Japan). The optical density values of the target bands were quantified relative to the level of β -actin using Gel-Pro analyzer 4.0 software (Media Cybernetics, USA).

Statistical analysis

Data were analyzed using SPSS 17.0 software (SPSS, Chicago,

IL, USA). Continuous variables were tested for normality using the Kolmogorov-Smirnov method. Normally distributed data are expressed as the mean \pm SD and were analyzed by one-way analysis of variance. Comparisons between two groups were conducted using the least significant difference test. Values of $P < 0.05$ were considered statistically significant.

Results

Pathological changes in hippocampi of newborn rats after HIBD

Rats in the HIBD only group exhibited rapid breathing, became agitated, and displayed tail wagging to the left side for 5–10 minutes after the animal model of HIBD was established. One hour after HIBD, rats became pale, had hypopnea, and presented with reduced locomotor activity and continuous convulsion. Gross examination revealed that the rat brain was pale beginning 6 hours after HIBD (**Figure 1A**). Compared with rats in the sham-operated group, rats in the HIBD only group had a higher brain wet weight 24 hours after the operation ($P < 0.01$; **Figure 1B**). Obvious brain swelling was detected at 24 hours and was worse 48 hours after HIBD. At 48 hours of HIBD, the frontal and parietal lobes appeared to be pale and displayed liquefactive necrosis, and the size of the injured cerebral hemisphere was larger than the contralateral side. Histological examination revealed that there was significant hippocampal neuronal damage 24 and 48 hours after HIBD (**Figure 1C**). Nissl staining revealed that rats in the HIBD only group had disturbed hippocampal structures, loss of neuronal cells, nuclear fragmentation, and Nissl body collapse (**Figure 1D**). Compared with that in the sham-operated group, the number of Nissl-positive neurons was greatly reduced in the HIBD only group ($P < 0.01$; **Figure 1E**).

Hippocampal LC3 and Beclin-1 expression in newborn rats with HIBD

To determine the involvement of autophagy in HIBD, the expression of the autophagy-related proteins LC3 and Beclin-1 were examined in the hippocampus of animals. The LC3 and beclin-1 mRNA levels were maintained at a relatively stable level in the hippocampus of rats in the sham-operated group. However, the LC3 mRNA level was significantly higher in rats in the HIBD only group than that in the sham-operated group 3 hours after HIBD induction. The LC3 mRNA level gradually increased and peaked 24 hours after HIBD ($P < 0.05$; **Figure 2A**). In addition, beclin-1 mRNA expression was significantly increased 12 hours and peaked 24 hours after surgery in the HIBD only group ($P < 0.05$, compared with the sham-operated group; **Figure 2B**). The enhanced levels of LC3 and beclin-1 mRNA expression were maintained until 48 hours after HIBD ($P < 0.05$, vs. sham-operated group). Immunohistochemical analysis revealed that the immunopositive staining for LC3 and Beclin-1 appeared to be enhanced at 24 hours in the HIBD only group (**Figure 2C, D**).

Hippocampal GluR1 and GluR2 expression in newborn rats after HIBD

To understand the involvement of the calcium-permeable

AMPA/kainate receptor-gated channel in HIBD, we examined the mRNA and protein expression levels of GluR1 and GluR2 in the hippocampal regions of rats after HIBD. As shown in **Figure 3**, the mRNA and protein levels of GluR1 were significantly elevated 12 hours, peaked 24 hours, and remained elevated 48 hours after HIBD ($P < 0.05$, vs. sham-operated group). By contrast, the mRNA and protein levels of GluR2 were markedly reduced beginning 3 hours after HIBD ($P < 0.05$, vs. sham-operated group), and the lowest mRNA and protein GluR2 expression levels were observed 12 hours after HIBD ($P < 0.05$, vs. sham-operated group). By contrast, no significant fluctuation in the expression of GluR1 or GluR2 was detected in the sham-operated group.

Effects of 3-MA and rapamycin on LC3 and Beclin-1 expression and on damage in the hippocampus of newborn rats with HIBD

The potential effects of autophagy on hippocampal damage were investigated using the autophagy inhibitor 3-MA and the autophagy stimulator rapamycin. As compared with the HIBD group, intraperitoneal injection of 3-MA 1 hour before surgery significantly decreased LC3 mRNA levels 1, 24, and 48 hours after HIBD ($P < 0.05$), and significantly decreased beclin-1 mRNA levels 24 and 48 hours after HIBD induction ($P < 0.05$; **Figure 4A, B**). However, pretreatment with rapamycin greatly increased mRNA levels of both LC3 and Beclin-1 24 and 48 hours after HIBD induction ($P < 0.05$, vs. HIBD). These data suggest that pharmacologically interfering with autophagy altered the mRNA levels of autophagy-related genes in the hippocampus following HIBD induction. In addition, 3-MA greatly attenuated the hippocampal damage induced by hypoxia-ischemia 24 hours after surgery (**Figure 4C**). By contrast, rapamycin greatly augmented HIBD-induced hippocampal injury, as severe neuronal apoptosis, necrosis, and cell loss were detected in the HIBD + rapamycin group.

Effects of 3-MA and rapamycin on hippocampal GluR1 and GluR2 expression in newborn rats with HIBD

The potential effects of autophagy on the expression of GluR1 and GluR2 were determined. The administration of 3-MA effectively blocked the HIBD-induced upregulation of glur1 mRNA 1, 24, and 48 hours after surgery; whereas rapamycin further elevated glur1 mRNA levels at the same times, compared with those for rats in the HIBD group ($P < 0.05$; **Figure 5A**). The glur2 mRNA levels 24 or 48 hours after surgery were markedly elevated by pretreatment with 3-MA but were significantly reduced 1, 24, or 48 hours after surgery by the administration of rapamycin ($P < 0.05$, vs. HIBD; **Figure 5B**). The administration of 3-MA reduced the ratio of glur1/glur2 that had been elevated by HIBD, whereas rapamycin further augmented the glur1/glur2 ratio (**Figure 5C**). Consistent results were obtained using the immunohistochemical analysis (**Figure 5D**).

Discussion

We found increased autophagic activity in the damaged hippocampus of rats with induced HIBD. The elevated ex-

pression levels of the autophagy-related proteins LC3 and Beclin-1 were accompanied by increased AMPAR GluR1 subunit expression levels but decreased GluR2 subunit levels. Pretreatment with an autophagy inhibitor attenuated hippocampal injury and blocked the HIBD-induced changes in GluR1 and GluR2 levels, whereas pretreatment with a stimulator of autophagy aggravated the HIBD-induced brain damage.

Autophagy is a physiological process critical for maintaining intracellular homeostasis by regulating protein turnover. In the nervous system, neuronal autophagy plays an essential role in mediating neuronal cell survival and death, while dysregulated autophagy contributes to several neurological diseases (Puyal et al., 2012; Yang et al., 2013). In the present study, cellular autophagy was activated following HIBD and was accompanied by increased LC3 and Beclin-1 levels. These observations are consistent with previous studies that showed the induction of autophagy after hypoxia-ischemia injury (Li et al., 2010; Xie et al., 2016). Autophagy activation tended to be more obvious 12–48 hours following HIBD, when severe hippocampal damage was also observed. However, we could not rule out the possibility that increased LC3 and Beclin-1 levels might also have reflected the accumulation of autophagosomes or autolysosomes caused by insufficient autophagic clearance. We also found that blocking autophagy with 3-MA significantly alleviated hippocampal damage, suggesting that autophagy may act as a pro-death mechanism in HIBD and that the inhibition of autophagic activity may suppress autophagic neuronal cell death upon injury. In contrast to our findings, Samokhvalov et al. (2008) demonstrated that blockade of autophagy sensitized cells to hypoxia injury in *C. elegans*, indicating a protective role of autophagy against insults. Our discrepant results may be explained by the use of different species of animal models.

Ion channels formed by AMPARs allow the influx of Ca^{2+} and are involved in the pathology of HIBD. In the present study, the marked upregulation of GluR1 and downregulation of GluR2 were detected 12–48 hours following HIBD. A recent study indicated that the exposure of cultured cortical cells to the neurotoxic chemicals methoxychlor and fenvalerate specifically decreased GluR2 expression, while the expression of other AMPAR subunits (GluR1, GluR3, and GluR4) remained unchanged (Umeda et al., 2016). This result suggests a crucial role of GluR2 in maintaining neuronal cell survival. The GluR2 subunit of AMPARs is distinct from the other subsets because AMPARs that lack GluR2 appear to be permeable to Ca^{2+} (Hollmann et al., 1991). Therefore, reduced GluR2 may augment cell death upon stimulation. We also observed that the altered expression of GluR1 and GluR2 was delayed after HIBD, which was consistent with the delayed hippocampal injury. These data were in accordance with previous findings showing the delayed, enhanced, and lasting activity of the GluR1 subunit in hippocampal slices cultured after transient anoxia/hypoglycemia (Quintana et al., 2006). Our findings show that normalized GluR1 and GluR2 expression levels may contribute to preventing HIBD in neonates, which may explain why AMPA antagonists have no immense neuroprotective potential following HI insult to the developing brain (Rocha-Ferreira and Hristova, 2016).

In addition, a significant reduction in the GluR1/GluR2 ratio

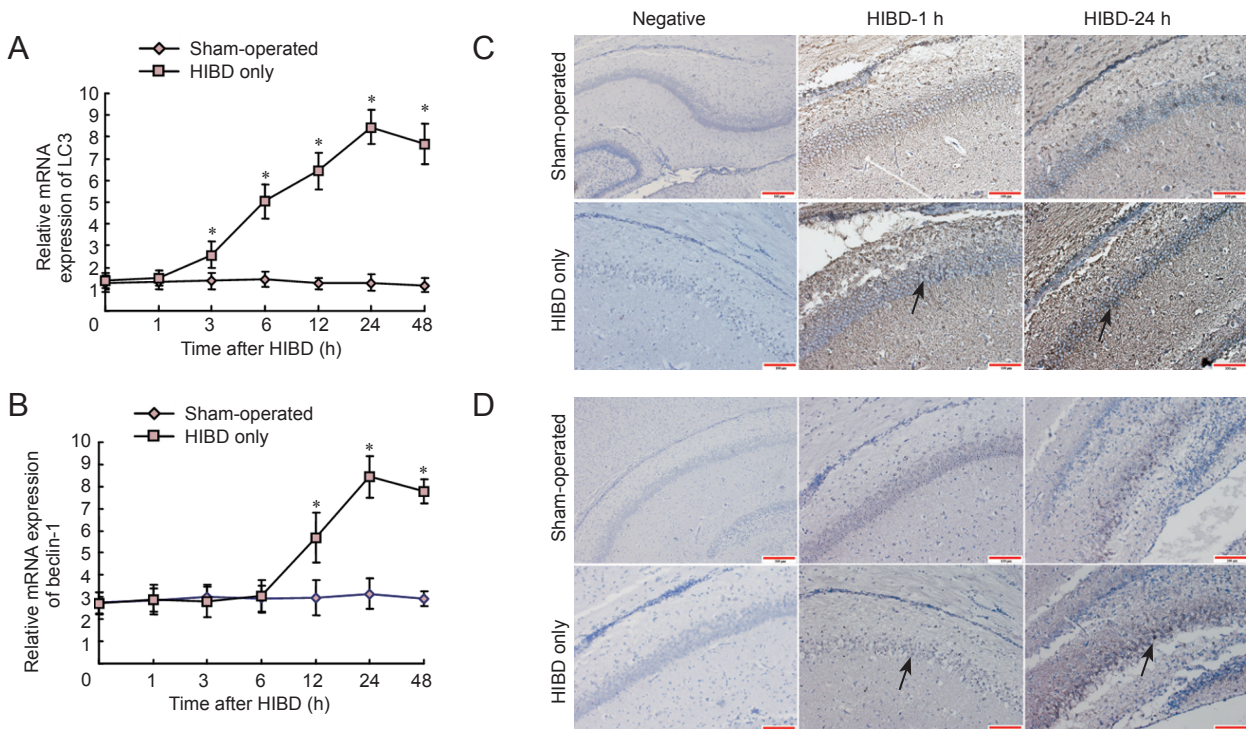


Figure 2 Expression of LC3 and Beclin-1 in the hippocampus following HIBD.

(A, B) The mRNA levels of LC3 (A) and beclin-1 (B) were measured by reverse transcription quantitative polymerase chain reaction. The mRNA expression was calculated relative to β -actin levels. Data are expressed as the mean \pm SD and were analyzed by one-way analysis of variance followed by the least significant difference test. $*P < 0.05$, vs. sham-operated group. (C, D) Hippocampal expression of LC3 (C) and Beclin-1 (D) as qualitatively determined using immunohistochemistry ($\times 200$) is higher in the HIBD group than that in the sham-operated group. Arrows represent immunoreactive cells. Three rats in each experimental group were examined at each time point. Negative: Control tissue processed without primary antibody. Scale bars in C and D: 100 μ m. h: Hour(s); LC3: light chain 3; HIBD: hypoxic-ischemic brain damage.

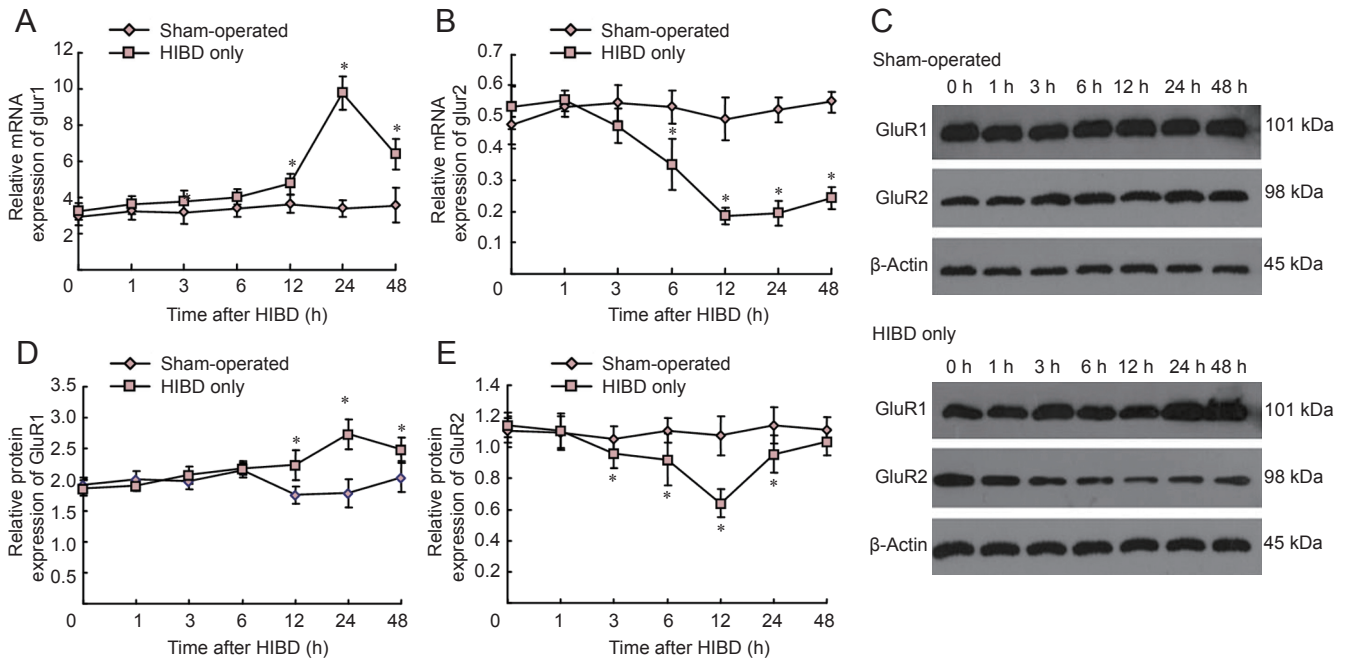


Figure 3 Expression of GluR1 and GluR2 in the hippocampus following HIBD.

(A, B) The mRNA levels of glur1 (A) and glur2 (B) were measured by reverse transcription quantitative polymerase chain reaction. The expression of mRNA was calculated relative to β -actin levels. (C) Protein expression was examined by western blot assay, and representative blots are presented. (D, E) The protein levels of GluR1 (D) and GluR2 (E) were calculated relative to β -actin levels. Data are expressed as the mean \pm SD and were analyzed by one-way analysis of variance followed by the least significant difference test. $*P < 0.05$, vs. sham-operated group. Three rats in each experimental group were included at each time point. h: Hour(s); HIBD: hypoxic-ischemic brain damage.

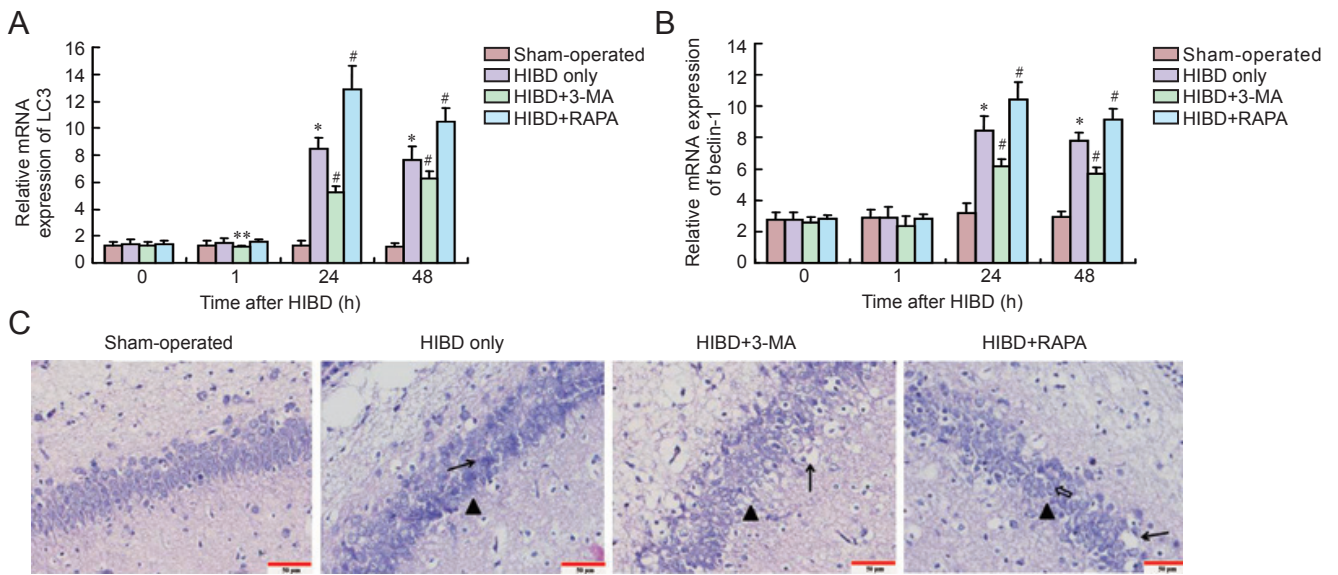


Figure 4 Effects of autophagy inhibition or stimulation on hippocampal damage following HIBD.

(A, B) The mRNA levels of LC3 (A) and beclin-1 (B) were measured by reverse transcription quantitative polymerase chain reaction. The expression of mRNA was calculated relative to β -actin levels. Data are expressed as the mean \pm SD and were analyzed by one-way analysis of variance followed by the least significant difference test. * $P < 0.05$, vs. sham-operated group; # $P < 0.05$, vs. HIBD group. (C) Hematoxylin-eosin staining of the hippocampal region 24 hours after surgery (magnification, $\times 400$). Scale bars: 50 μ m. Black arrows show cell swelling; arrowheads show loosely distributed cells; the open arrow indicates damaged cell. Three rats in each experimental group were included at each time point. 3-MA: 3-Methyladenine; RAPA: rapamycin; h: hour(s); LC3: light chain 3; HIBD: hypoxic-ischemic brain damage.

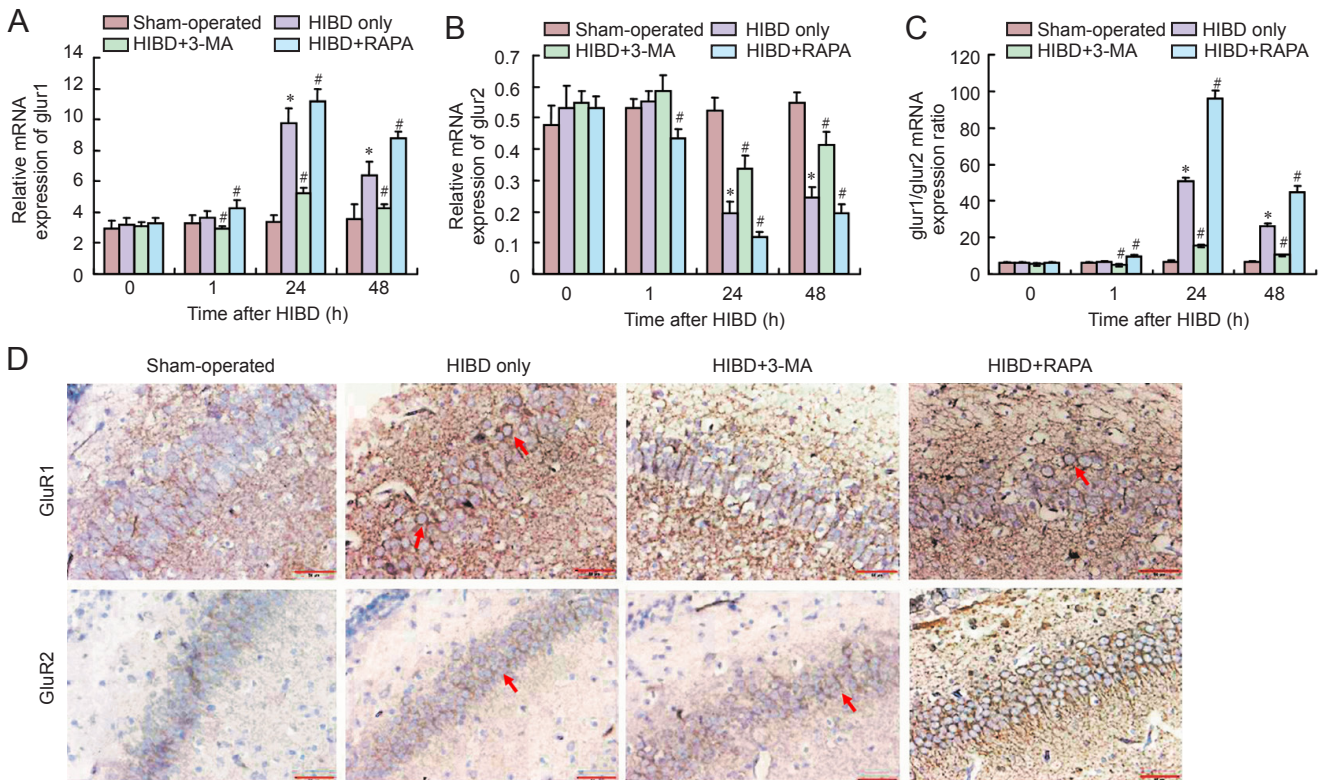


Figure 5 Effects of 3-MA and RAPA on GluR1 and GluR2 in the hippocampus following HIBD.

(A, B) The mRNA levels of glur1 (A) and glur2 (B) were measured by reverse transcription quantitative polymerase chain reaction 24 hours after surgery. The expression of mRNA was calculated relative to β -actin levels. (C) glur1/glur2 ratios over time. Data are expressed as the mean \pm SD and were analyzed by one-way analysis of variance followed by the least significant difference test. * $P < 0.05$, vs. sham-operated group; # $P < 0.05$, vs. HIBD group. (D) Immunohistochemical analysis of GluR1 and GluR2 expression in the hippocampus ($\times 400$). Arrows show positive expression. Scale bars: 50 μ m. Three rats in each experimental group were included at each time point. 3-MA: 3-Methyladenine; RAPA: rapamycin; h: hour(s); HIBD: hypoxic-ischemic brain damage.

was found in HIBD animals pretreated with the autophagy inhibitor 3-MA. By contrast, pretreatment with an autophagy stimulator prior to HIBD resulted in a marked enhancement in the GluR1/GluR2 ratio. The autophagy inhibitory and stimulatory effects of 3-MA and rapamycin, respectively, were confirmed here by determining the expression levels of LC3 and Beclin-1 in the hippocampus of rats. A previous study demonstrated that rapamycin inhibited the mammalian target of rapamycin (mTOR) pathway while autophagy was activated, and this contributed to the reduced AMPAR expression in the synapses of cortical neurons (Wang et al., 2006). The mTOR and autophagy pathways are novel targets for interfering with HIBD (Chen et al., 2012). It is plausible that autophagy induction leads to the excessive degradation of GluR2, which is associated with neuronal toxicity. Autophagy inhibition by 3-MA in the present study contributed to the restored GluR2 expression in hippocampal neurons. Moreover, because 3-MA inhibits phosphoinositide 3-kinase (PI3K) signaling (Blommaert et al., 1997), cross talk may occur between GluR1/GluR2 and the PI3K-Akt-mTOR signaling pathway. However, the underlying correlation between GluR1/GluR2 and the PI3K-Akt-mTOR pathways needs to be further investigated.

In summary, autophagy inhibition favored neuronal survival in the hippocampus of rats following HIBD, whereas autophagy stimulation augmented neuronal death. The neuroprotective role of autophagy blockade may be associated with a reduced GluR1/GluR2 ratio in the hippocampus after HIBD. The results of our study support the approach of interfering with autophagic activity for preventing neuronal damage after HIBD. Nevertheless, the precise association between autophagy and AMPARs in regulating neuronal survival and death in the brains of neonates subjected to HIBD remains to be further clarified.

Author contributions: LXX and XJT had primary responsibility for study design, data analysis and manuscript preparation. YYY participated in hematoxylin-eosin staining and prepared the manuscript. ML and MFJ helped with model establishment and conducted immunohistochemistry. PM and XD helped in the establishment of the HIBD model and in conducting the western blot assay. YW participated in qPCR analysis. YHL helped in the data analysis. BS and XF contributed to the study design and provided valuable suggestions for conducting the experiments. All authors read and approved the final version of the paper.

Conflicts of interest: None declared.

Plagiarism check: This paper was screened twice using CrossCheck to verify originality before publication.

Peer review: This paper was double-blinded and stringently reviewed by international expert reviewers.

References

Blommaert EF, Krause U, Schellens JP, Vreeling-Sindelárová H, Meijer AJ (1997) The phosphatidylinositol 3-kinase inhibitors wortmannin and LY294002 inhibit autophagy in isolated rat hepatocytes. *Eur J Biochem* 243:240-246.

Chen H, Qu Y, Tang B, Xiong T, Mu D (2012) Role of mammalian target of rapamycin in hypoxic or ischemic brain injury: potential neuroprotection and limitations. *Rev Neurosci* 23:279-287.

Dixon BJ, Reis C, Ho WM, Tang J, Zhang JH (2015) Neuroprotective strategies after neonatal hypoxic ischemic encephalopathy. *Int J Mol Sci* 16:22368-22401.

Gainey MA, Hurvitz-Wolff JR, Lambo ME, Turrigiano GG (2009) Synaptic scaling requires the GluR2 subunit of the AMPA receptor. *J Neurosci* 29:6479-6489.

Guo H, Zhou H, Lu J, Qu Y, Yu D, Tong Y (2016) Vascular endothelial growth factor: an attractive target in the treatment of hypoxic/ischemic brain injury. *Neural Regen Res* 11:174-179.

Hollmann M, Hartley M, Heinemann S (1991) Ca²⁺ permeability of KA-AMPA-gated glutamate receptor channels depends on subunit composition. *Science* 252:851-853.

Klionsky DJ, Abdelmohsen K, Abe A, Abedin MJ, Abeliovich H, Acevedo Arozena A, Adachi H, Adams CM, Adams PD, Adeli K, Adhihetty PJ, Adler SG, Agam G, Agarwal R, Aghi MK, Agnello M, Agostinis P, Aguilar PV, Aguirre-Ghiso J, Airolidi EM, et al. (2016) Guidelines for the use and interpretation of assays for monitoring autophagy (3rd edition). *Autophagy* 12:1-222.

Li Q, Li H, Roughton K, Wang X, Kroemer G, Blomgren K, Zhu C (2010) Lithium reduces apoptosis and autophagy after neonatal hypoxia-ischemia. *Cell Death Dis* 1:e56.

Liu SJ, Savtchouk I (2012) Ca(2+) permeable AMPA receptors switch allegiances: mechanisms and consequences. *J Physiol* 590:13-20.

Livak KJ, Schmittgen TD (2001) Analysis of relative gene expression data using real-time quantitative PCR and the 2(-Delta Delta C(T)) Method. *Methods* 25:402-408.

Matsuda S, Miura E, Matsuda K, Kakegawa W, Kohda K, Watanabe M, Yuzaki M (2008) Accumulation of AMPA receptors in autophagosomes in neuronal axons lacking adaptor protein AP-4. *Neuron* 57:730-745.

Patel Shyama D, Pierce L, Ciardiello Amber J, Vannucci Susan J (2014) Neonatal encephalopathy: pre-clinical studies in neuroprotection. *Biochem Soc Trans* 42:564-568.

Perlman M, Shah PS (2011) Hypoxic-ischemic encephalopathy: challenges in outcome and prediction. *J Pediatr* 158:e51-e54.

Puyal J, Ginet V, Grishchuk Y, Truttmann AC, Clarke PG (2012) Neuronal autophagy as a mediator of life and death: contrasting roles in chronic neurodegenerative and acute neural disorders. *Neuroscientist* 18:224-236.

Quintana P, Alberi S, Hakkoum D, Muller D (2006) Glutamate receptor changes associated with transient anoxia/hypoglycaemia in hippocampal slice cultures. *Eur J Neurosci* 23:975-983.

Rocha-Ferreira and Hristova (2016) Plasticity in the neonatal brain following hypoxic-ischaemic injury. *Neural Plast* 2016:4901014.

Samokhvalov V, Scott BA, Crowder CM (2008) Autophagy protects from hypoxic injury in *C. elegans*. *Autophagy* 4:1034-1041.

Shankaran S (2012) Hypoxic-ischemic encephalopathy and novel strategies for neuroprotection. *Clin Perinatol* 39:919-929.

Shehata M, Matsumura H, Okubo-Suzuki R, Ohkawa N, Inokuchi K (2012) Neuronal stimulation induces autophagy in hippocampal neurons that is involved in AMPA receptor degradation after chemical long-term depression. *J Neurosci* 32:10413-10422.

Shi SH, Hayashi Y, Esteban JA, Malinow R (2001) Subunit-specific rules governing AMPA receptor trafficking to synapses in hippocampal pyramidal neurons. *Cell* 105:331-343.

Tang XJ, Xing F (2013) Calcium-permeable AMPA receptors in neonatal hypoxic-ischemic encephalopathy (Review). *Biomed Rep* 1:828-832.

Umeda K, Kotake Y, Miyara M, Ishida K, Sanoh S, Ohta S (2016) Methoxychlor and fenvalerate induce neuronal death by reducing GluR2 expression. *J Toxicol Sci* 41:255-264.

Vannucci RC, Vannucci SJ (1997) A model of perinatal hypoxic-ischemic brain damage. *Ann N Y Acad Sci* 835:234-249.

Wang Y, Barbaro MF, Baraban SC (2006) A role for the mTOR pathway in surface expression of AMPA receptors. *Neurosci Lett* 401:35-39.

Xie C, Ginet V, Sun Y, Koike M, Zhou K, Li T, Li H, Li Q, Wang X, Uchiyama Y, Truttmann AC, Kroemer G, Puyal J, Blomgren K, Zhu C (2016) Neuroprotection by selective neuronal deletion of Atg7 in neonatal brain injury. *Autophagy* 12:410-423.

Yang Y, Coleman M, Zhang L, Zheng X, Yue Z (2013) Autophagy in axonal and dendritic degeneration. *Trends Neurosci* 36:418-428.

Yao Y, Zheng XR, Zhang SS, Wang X, Yu XH, Tan JL, Yang YJ (2016) Transplantation of vascular endothelial growth factor-modified neural stem/progenitor cells promotes the recovery of neurological function following hypoxic-ischemic brain damage. *Neural Regen Res* 11:1456-1463.

Zalewska T, Jaworska J, Ziemka-Nalecz M (2015) Current and experimental pharmacological approaches in neonatal hypoxic-ischemic encephalopathy. *Curr Pharm Des* 21:1433-1439.

Copyedited by Smith T, Robens J, Yu J, Li CH, Qiu Y, Song LP, Zhao M